COMPDYN 2017
6th ECCOMAS Thematic Conference on
Computational Methods in Structural Dynamics and Earthquake Engineering
M. Papadrakakis, M. Fragiadakis (eds.)
Rhodes Island, Greece, 15–17 June 2017

GEOTECHNICAL SEISMIC ISOLATION USING EPS GEOFOAM AROUND PILES

Xenia A. Karatzia[1] **and George E. Mylonakis**[1,2]

[1] University of Patras
Dept. of Civil Engineering, Rio 26500, Greece
{xkar, mylo}@upatras.gr

[2] University of Bristol
Dept. of Civil Engineering, Queens Building, Bristol BS8 1TR, U.K.
g.mylonakis@bristol.ac.uk

Keywords: Geotechnical Isolation, Pile Foundations, Bridge Pier, EPS Geofoam, Period Elongation.

Abstract. *The feasibility of a new geotechnical seismic isolation system for pile-supported structures, such as bridge piers on monopiles, is investigated. The isolation system utilizes a soft annular zone of viscoelastic material, such as EPS geofoam, around the upper part of the pile. The presence of the EPS elongates the fundamental natural period of the structure and also modifies its damping. For simplicity and as a proof of concept, the superstructure is considered a simple oscillator. Based on a dynamic Winkler model for pile-soil interaction, the problem is treated analytically leading to a simple design-oriented analysis method. Closed-form solutions are obtained for: (a) the lateral stiffness of the structure-foundation system, (b) the corresponding fundamental period, and (c) the overall damping. Numerical analyses in the frequency domain by means of the computer code SPIAB verify the above analytical predictions. Analyses in the time domain are also carried out to examine the effect of geofoam on the dynamic response. Results in terms of base shear, maximum pile bending moment, and displacement at deck level are presented in dimensionless form, allowing for quantification of the effect of geofoam on seismic performance. It is shown that the presence of geofoam around the pile can reduce the seismic demand, rendering the proposed method a promising, inexpensive alternative to structural protective systems.*

1 INTRODUCTION

The objective of this paper is to study an alternative, geotechnically-oriented method of seismic protection for pile-supported structures, using industrial materials such as EPS geofoam, around the upper part of the pile, for reducing seismic forces. The proposed system can be classified in the realm of Geotechnical Seismic Isolation (GSI).

The concept of GSI has attracted significant research interest as an alternative to conventional Structural Seismic Isolation approaches. Although the idea has existed for a long time, the term GSI was formally introduced by Tsang [1] to describe isolation systems associated with the soil under the foundation. The first relevant innovative idea was put forth by Kavazanjian et al. [2] and Yegian and Lahlaf [3], who worked independently, with reference to the use of geosynthetic materials as a cost-effective frictional base isolation for structures. Later, Yegian and Kadakal [4] proposed placing a smooth synthetic liner underneath the foundation of a structure to dissipate earthquake energy. Along the same lines, Yegian and Catan [5] examined the use of geotextiles between soil layers to reduce horizontal ground motions at the expense of increased soil compliance. Later, Tsang [6] suggested soil improvement around the foundation of buildings by means of rubber-soil mixtures (RSM) for absorbing seismic energy while Xiong et al. [7,8] investigated, via shaking table tests, the dynamic performance of GSI with rubber-soil mixtures and concluded that the response of the system with the isolation is generally inferior to that of a foundation underlain by pure sand. These applications, although interesting from an academic view point, do not provide control of foundation settlements and, therefore, do not fulfill design requirements for important structures.

In the present study, a new geotechnical isolation system for pile-supported bridge piers using elastic inclusions, such as EPS geofoam, around piles is proposed. EPS Geofoam [9] is a very promising material for such purposes due to well-known mechanical behavior, energy dissipation capability, ease of installation and replacement, and low cost. An important feature is that EPS possesses sufficient compressive and shear strength to undertake the lateral soil pressures, while at the same time renders the foundation flexible, since the geofoam-soil stiffness ratio is small. Additionally, the dynamic material properties of EPS have been extensively investigated in recent times [10,11].

It is demonstrated that geofoam around the pile operates as an isolation mechanism, increasing the fundamental natural period of the system and decreasing the seismically-induced forces. The problem is solved analytically based on dynamic Winkler considerations leading to closed-form expressions for the compliance, fundamental natural period and the effective damping of the superstructure-foundation system. Numerical analyses in frequency and time-domain are conducted to examine the influence of the geometrical and mechanical properties of the EPS coat on the vibrational properties of the system, the maximum base shear and the pile bending moment. The increase in deck displacements due to the presence of geofoam is, thereby, explored.

2 PROBLEM DEFINITION

Fig. 1a depicts a cantilever structure which can be viewed as an idealization of an actual bridge pier. The model involves a single-column bent supported on a single pile which is enhanced with a compressible cylindrical EPS coat, founded in a homogeneous soil stratum over bedrock. The structure is subjected to vertically propagating S-waves imposed at bedrock level. The pile is modelled as a linearly viscoelastic solid cylindrical beam of diameter d, Young's modulus E_p and linear hysteretic damping β_p. The geofoam inclusion has thickness t, length D_e, Young's modulus E_{inc}, Poisson's ratio ν_{inc} and hysteretic damping β_{inc}. The super-

structure is essentially a single-degree-of-freedom oscillator of height H and same diameter as that of the pile, and mass m. The soil is modeled as a linearly viscoelastic medium of Young's modulus E_s, Poisson's ratio v_s, mass density ρ_s and linear hysteretic damping β_s. The soil, pile, inclusion and structural properties used in the analyses are given in Table 1.

Considering same material properties for the column and the pile and using standard dimensional analysis, the following dimensionless ratios can be defined for describing the response: the stiffness ratios E_{inc}/ E_s and E_p / E_s, the dimensionless inclusion thickness t/d, the slenderness ratio H/d and the embedment depth of the geofoam D_e / L_a (L_a being the familiar "active" pile length).

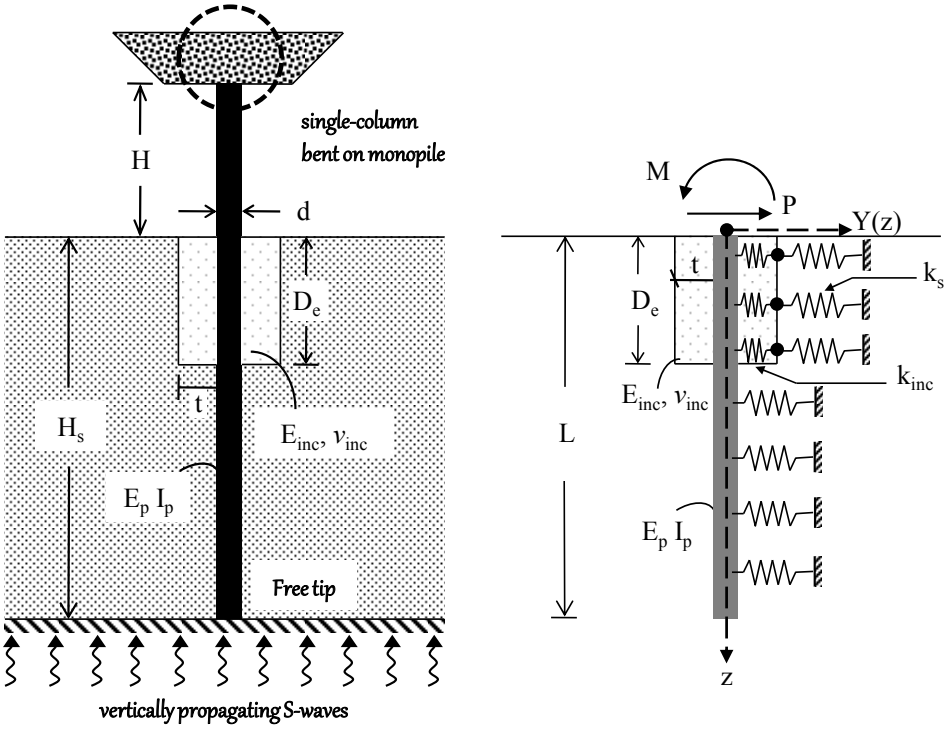

Figure 1: a) Bridge pier founded on a single pile enhanced with a geofoam coat, b) Modeling approach of soil-geofoam-pile interaction.

Soil	Pile	Inclusion	Column bent
$E_s = 2.5\times10^4$ *kP*a $\rho_s = 2$ *Mg* / m^3 $\beta_s = 10$ % $v_s = 0.4$	$E_p = 2.5\times10^7$ *kP*a $d = 1$ *m* $L = 20$ *m* $\rho_p = 2.5$ *Mg* / m^3 $\beta_p = 5$ %	$E_{inc} / E_s = 0.01 - 1$ $\beta_{inc} = 10$ % $v_{inc} = 0.15$ $t / d = 0.25, 0.5, 1$ $D_e / L_a = 0.25, 0.5, 1$	$E = 2.5\times10^7$ *kP*a $d = 1$ *m* $\beta = 5$ % $H / d = 5, 10, 20$

Table 1: Soil, pile, inclusion and column bent properties utilized

3 PROPOSED ANALYTICAL SOLUTION

3.1 Stiffness and damping coefficients of a pile provided with inclusion

Fig. 1b depicts the model employed for simulating the soil-inclusion-pile interaction. The lateral stiffness of the inclusion and the soil are denoted with k_{inc} and k_s, respectively. The problem of horizontal soil reaction of a cylindrical pile segment with a compressible annular zone of finite thickness has been studied and closed-form solutions for the stiffness of the inclusion are available [11-13]. Therefore, the stiffness coefficient in case of a pile enhanced with an elastic or viscoelastic annular soft zone is given by the relationship

$$k_{inc} = \left(\frac{4\pi E_{inc}}{1+v_{inc}}\right) \frac{\left(1-v_{inc}\right)\left[\left(2t/d+1\right)^2+1\right]}{\left(1-2v_{inc}\right)^2\left[\left(2t/d+1\right)^2-1\right]+\left(3-4v_{inc}\right)\left[\left(2t/d+1\right)^2+1\right]\ln\left(2t/d+1\right)} \tag{1}$$

with E_{inc} and v_{inc} being the Young's modulus and the Poisson's ratio of the inclusion, respectively; t is the thickness of the inclusion and d the pile diameter. Eq.(1) refers to perfectly smooth interfaces between pile and inclusion, and between inclusion and soil.

k_s represents the value of the soil spring constant, typically expressed as $k_s = \delta E_s$ with δ being a dimensionless coefficient typically ranging from 1 to 2.5 depending on soil inhomogeneity, pile-soil stiffness contrast and boundary conditions at the pile head [14-16]. A value of 2 was adopted for the herein reported analyses.

Using the Winkler hypothesis, the compliance of the inclusion-soil system is described through a pair of springs attached in a series (Fig. 1b). Accordingly, the stiffness up to depth D_e is

$$\hat{k}_s = k_{inc}\frac{1}{1+\left(k_{inc}/k_s\right)} \tag{2}$$

Note that, this is an approximate solution as the distortion of the foam-soil interface is neglected, leading to a somewhat stiffer system. Nevertheless, because the soil material is typically much stiffer than the inclusion ($k_{inc}/k_s \le 10^{-1}$) the overall stiffness practically coincides with that of the inclusion [12,13].

Evidently, a two-layer geometry is obtained, which consists of an upper zone of thickness D_e, stiffness $\hat{k}_s$ and Winkler parameter λ_1 followed by a second zone of stiffness k_s and Winkler parameter λ_2. The values of λ_1 and λ_2 are obtained from the familiar equations

$$\lambda_1 = \left(\frac{\hat{k}_s}{4E_pI_p}\right)^{1/4} \quad , \quad \lambda_2 = \left(\frac{k_s}{4E_pI_p}\right)^{1/4} \tag{3}$$

The average value of λ_1 and λ_2 over the active pile length L_a defines a Winkler shape parameter [17]

$$\mu = \frac{D_e}{L_a}\lambda_1 + \frac{1}{L_a}\left(1-\frac{D_e}{L_a}\right)\lambda_2 \tag{4}$$

By employing the relation $\mu \cong 2.5 / L_a$ [18], the active pile length can be expressed as a function of the inclusion length D_e

$$L_a/D_e = \frac{2.5D_e^{-1}+\left(\lambda_2-\lambda_1\right)}{\lambda_2} \tag{5}$$

Utilizing the virtual work method and a set of pertinent shape functions for pile deflection [16,17,19,22], the static stiffness coefficients K_{hh}, K_{rr} and K_{hr} corresponding to swaying, rocking and cross-swaying-rocking, respectively, at the pile head can be readily determined. The stiffness terms corresponding to a two-layer soil are [22]

$$K_{hh} = E_p I_p \mu^3 \left(1+s_{hh}\right), \quad K_{rr} = \frac{3}{2} E_p I_p \mu \left(1+s_{rr}\right), \quad K_{hr} = E_p I_p \mu^2 \left(1+s_{hr}\right) \tag{6}$$

where

$$s_{hh} = \frac{16\delta}{\pi} \frac{\hat{k}_s}{k_s} \left(\frac{E_p}{E_s}\right)^{-1} \left(\frac{1}{\mu d}\right)^4 \left\{3 - \left(1 - \frac{k_s}{\hat{k}_s}\right) e^{-2\mu D_e} \left[2 + \cos\left(2\mu D_e\right) + \sin\left(2\mu D_e\right)\right]\right\} \tag{7}$$

$$s_{rr} = \frac{16\delta}{3\pi} \frac{\hat{k}_s}{k_s} \left(\frac{E_p}{E_s}\right)^{-1} \left(\frac{1}{\mu d}\right)^4 \left\{1 - \left(1 - \frac{k_s}{\hat{k}_s}\right) e^{-2\mu D_e} \left[2 - \cos\left(2\mu D_e\right) + \sin\left(2\mu D_e\right)\right]\right\} \tag{8}$$

$$s_{hr} = \frac{16\delta}{\pi} \frac{\hat{k}_s}{k_s} \left(\frac{E_p}{E_s}\right)^{-1} \left(\frac{1}{\mu d}\right)^4 \left\{1 - \left(1 - \frac{k_s}{\hat{k}_s}\right) e^{-2\mu D_e} \left[1 + \sin\left(2\mu D_e\right)\right]\right\} \tag{9}$$

Besides lowering stiffness, the inclusion also changes the effective damping of the system. The effective damping is controlled by the inclusion-to-soil stiffness contrast (k_{inc}/k_s) through the expression

$$\hat{\beta}_s = \left[\frac{1}{1+\left(k_{inc}/k_s\right)}\right] \beta_{inc} + \left[\frac{\left(k_{inc}/k_s\right)}{1+\left(k_{inc}/k_s\right)}\right] \left(\beta_s + \beta_r\right) \tag{10}$$

β_{inc}, β_s and β_r being inclusion damping, soil material damping and radiation damping, respectively; the terms in brackets can be interpreted as weight factors. The damping coefficients pertaining to a pile foundation are obtained according to the following mixing rules [20]

$$\beta_{hh} = \frac{3}{4}\hat{\beta}_s + \frac{1}{4}\beta_p, \quad \beta_{rr} = \frac{1}{4}\hat{\beta}_s + \frac{3}{4}\beta_p, \quad \beta_{hr} = \frac{1}{2}\hat{\beta}_s + \frac{1}{2}\beta_p \tag{11}$$

β_{hh}, β_{rr} and β_{hr} being the damping coefficients at the pile head related to swaying, rocking and cross-swaying-rocking, respectively. Note that the influence of radiation damping coefficient is small in the presence of an EPS coat and is ignored in the ensuing analyses.

3.2 Vibrational properties of the pier-pile-inclusion-soil system

The overall displacement of the flexible bridge pier of Fig. 1 can be viewed as the superposition of two distinct components: (1) a horizontal displacement and a rotation due to coupling between foundation swaying and rocking, and (2) an additional displacement reflecting the compliance of the superstructure. Hence, the compliances of the foundation and the superstructure can be regarded as a pair of complex-valued springs assembled in parallel under a common imposed load. Accordingly, the total stiffness of the system, K_t, is given by the simple combination formula

$$K_t \cong \frac{K_f K}{K_f + K} \tag{12}$$

where K is the stiffness of a fixed-base bridge pier while K_f is the corresponding stiffness of a rigid bridge pier on a compliant pile foundation, given by [14]

$$K_f \cong \frac{K_{hh} K_{rr} - K_{hr}^2}{K_{rr} + (w+1) H K_{hr} + w H^2 K_{hh}} \tag{13}$$

In the above expression, K_{hh}, K_{rr} and K_{hr} stand for the swaying, rocking and cross-swaying-rocking impedances at the pile head and H denotes the pier height. Parameter w accounts for the effect of fixity conditions at the top of the column bent (w = 1, 0.5 for moment free and clamped condition, respectively). In case of a pile provided with an EPS coat, Eqs. (6) – (9) should be employed in Eq. (13) for obtaining the stiffness of the system. By substituting the stiffness terms with their complex impedance values, $K_{hh}^* = K_{hh}(1 + 2i\beta_{hh})$, $K_{rr}^* = K_{rr}(1 + 2i\beta_{rr})$ and $K_{hr}^* = K_{hr}(1 + 2i\beta_{hr})$ and after some tedious algebra, the stiffness and damping coefficients of a rigid bridge pier on a compliant pile foundation are derived from the exact expressions [21-23]

$$K_f = HK_{hr} \frac{K_{hh}K_{rr}\left[\chi_1 + \chi_2 + 2\left(-\chi_3 + 4\chi_4\beta_{hr}\right)\right] - K_{hr}^2\left[\chi_5 + 8\chi_6\beta_{hr} + \chi_7\left(1 - 4\beta_{hr}^2\right)\right]}{\left(H^2K_{hh} + 2HK_{hr} + K_{rr}\right)^2 + 4\left(H^2K_{hh}\beta_{hh} + 2HK_{hr}\beta_{hr} + K_{rr}\beta_{rr}\right)^2} \tag{14}$$

$$\beta_f = \frac{\chi_1\beta_{rr} + \chi_2\beta_{hh} + 2\left(\chi_3\beta_{hr} + \chi_4\right) - \frac{K_{hr}^2}{K_{hh}K_{rr}}\left[\chi_5\beta_{hr} + 2\chi_7\beta_{hr} - \chi_6\left(1 - 4\beta_{hr}^2\right)\right]}{\chi_1 + \chi_2 + 2\left(-\chi_3 + 4\chi_4\beta_{hr}\right) - \frac{K_{hr}^2}{K_{hh}K_{rr}}\left[\chi_5 + 8\chi_6\beta_{hr} + \chi_7\left(1 - 4\beta_{hr}^2\right)\right]} \tag{15}$$

$\chi_1, \chi_2, \chi_3, \chi_4, \chi_5, \chi_6, \chi_7$ being dimensionless quantities given in the Appendix.

The fundamental period of the superstructure-pile-inclusion-soil system is given by

$$\frac{\hat{T}}{T} = \sqrt{1 + \frac{K}{\hat{K}_f}} \tag{16}$$

with T ($= 2\pi\sqrt{(m/K)}$) being the fixed-base fundamental period of the pier. In the same vein, the effective damping of the system is determined as [22]

$$\hat{\beta} = \frac{1}{1 + \frac{1 + (2\beta)^2}{1 + \left(2\hat{\beta}_f\right)^2}\left(\frac{K}{\hat{K}_f}\right)}\beta + \frac{1}{\frac{1 + \left(2\hat{\beta}_f\right)^2}{1 + (2\beta)^2}\left(\frac{\hat{K}_f}{K}\right) + 1}\hat{\beta}_f \tag{17}$$

β being the damping ratio of the superstructure.

To assess the impact of the inclusion on the fundamental period of the flexible bridge pier-pile-soil system, the following closed-form equation is obtained

$$\frac{\hat{T}}{\tilde{T}} = \sqrt{\frac{1 + \left(K / \hat{K}_f\right)}{1 + \left(K / \tilde{K}_f\right)}} \tag{18}$$

where $\tilde{K}_f$ is the stiffness of the flexible pier-pile-soil system considering only the effect of soil-structure interaction without the EPS coat. In this case Eqs. (12) and (13) still hold with

the stiffness coefficients atop the pile head being $K_{hh} = 4E_pI_p\lambda^3$, $K_{rr} = 2E_pI_p\lambda$ and $K_{hr} = 2E_pI_p\lambda^2$, corresponding to homogeneous soil conditions, with Winkler parameter λ being equal to λ_2.

3.3 Determination of inertial forces based on the response spectrum

Based on the familiar response spectrum method, the peak earthquake response of a single-degree-of-freedom system can be obtained from the spectral acceleration $S_A(\hat{T}, \hat{\beta})$ corresponding to the natural oscillation period $\hat{T}$ and an appropriate modification according to the effective damping ratio $\hat{\beta}$ [24]. The modification due to kinematic effects related to soil-pile interaction, is neglected in the present simple analysis. Accordingly, the base shear V_b in the pier and the corresponding overturning moment M_b are

$$V_b = m\, S_A\left(\hat{T}, \hat{\beta}\right) \tag{19}$$

$$M_b = H\, V_b \tag{20}$$

3.4 A brief discussion on the proposed isolation method

From Eqs. (16) and (18), it is obvious that the inclusion acts as a fundamental base-isolation mechanism increasing the natural period of the pier. In the context of SSI, the flexibility of the foundation increases and, thus, the fundamental period of the system becomes longer than the fixed-base natural period. In the realm of a response spectrum analysis, the increase in fundamental period leads to a change in spectral acceleration and, hence, in design base shear, as shown in Fig. 2.

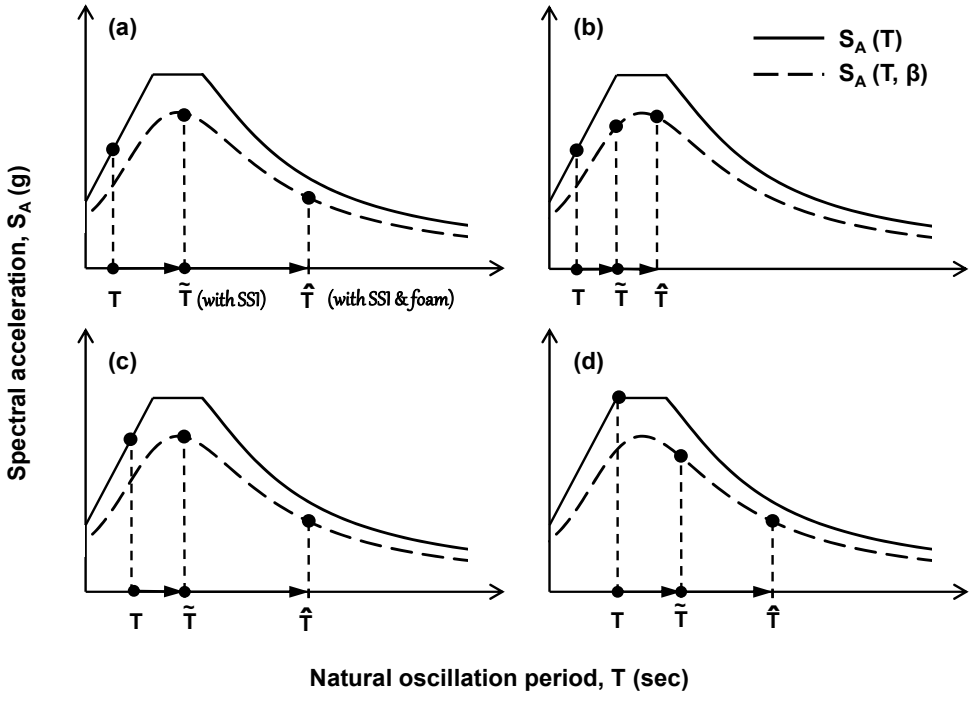

Figure 2: Period lengthening of the bridge pier system due to soil-structure-interaction and use of geofoam; T and β indicate the natural oscillation period and the effective damping of the system.

Principally, the effect of SSI on the design forces is related to the slope of the response spectrum: a positive slope results in an increased base shear while a negative slope results in a

reduced base shear [20]. The use of EPS coat around the pile makes the system even more flexible and its fundamental period longer than the classical SSI period (without EPS coat) of the pier. From the elastic design spectrum of Fig. 2, it is evident that this period shift can lead to an increase or decrease in seismic demand depending on the circumstances.

A common problem in isolation methods lies in the increased displacements resulting from the increase in period, since the latter is shifted in or near the displacement-sensitive region of the spectrum. This means that structural displacements should be checked to be within acceptable limits.

4 PARAMETRIC STUDY AND COMPARISONS WITH SPIAB

The system period normalized with the fixed-base period, $\hat{T} / T$, (Eq. 16) and the effective damping ratio normalized with that of the structure, $\hat{\beta} / \beta$, (Eq. 17) are plotted against the inclusion-soil stiffness contrast E_{inc} / E_s. Figs. 3 and 4 depict the influence of the dimensionless length, D_e / L_a, and thickness, t / d, of the EPS coat, the slenderness ratio H / d and the pile-soil stiffness contrast E_p / E_s on the vibrational properties of the interacting system. The following observations can be made [22-23]:

1. As the E_{inc} / E_s ratio decreases, the period lengthening is greater.
2. An increase in t / d ratio seems to slightly increase the fundamental period.
3. The variation in D_e / L_a ratio seems to be of secondary importance; however the use of a short inclusion can have a great impact on the system period. As a matter of fact, the period of squat structures is affected by the use of the EPS coat, with the natural period increasing considerably, while the period of tall slender structures is less sensitive to the addition of EPS.
4. The system period increases with increasing E_p / E_s ratio.
5. The effective damping of the system seems to be marginally affected by the variation in the value of the parameters studied.

It is pointed out that, according to experimental results [10], the damping ratio of geofoam may reach 10% at strains on the order of 10^{-1}, which implies that geofoam may provide sufficient energy dissipation for isolation purposes. Thus, the use of $\beta_{inc} = 10\%$ in the present study seems to be a reasonable assumption. It is also noted that the use of EPS coat may increase or decrease the overall damping of the system. In this analysis, where $\beta_s = 10\%$ is considered the effective damping seems to be unaffected by β_{inc}. If a value of $\beta_{inc} = 5\%$ was employed, the effective damping of the system would naturally decrease. Note that no radiation damping has been considered in the analyses, yet its influence is not expected to be dominant.

It is also noted that the plot of Eq. (18) exhibits similar trends with the plot of Eq. (16) with the difference that the ordinates of curves for the fundamental period of the system naturally attain values larger than 1 (not shown).

On the same graphs, numerical results obtained by means of the computer code SPIAB [17] are shown, in which the problem is solved in an exact manner in the realm of Winkler theory. Evidently, comparison between the proposed analytical solution and the numerically evaluated results is satisfactory.

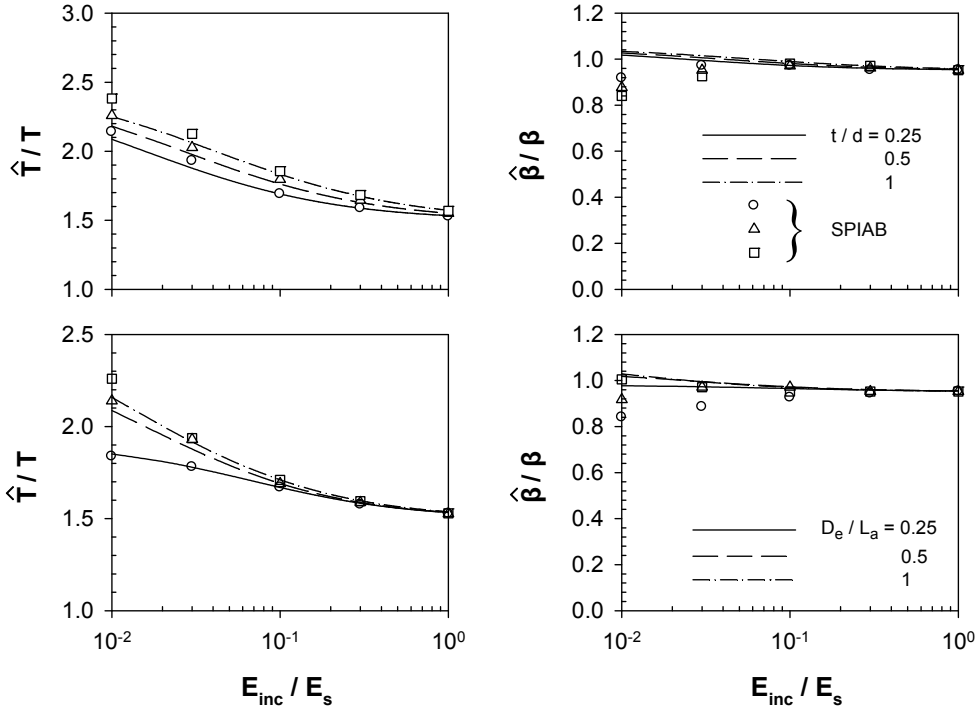

Figure 3: System period and effective damping as function of inclusion-soil stiffness ratio E_{inc}/E_s: Influence of dimensionless thickness t/d and length of EPS coat D_e/L_a.

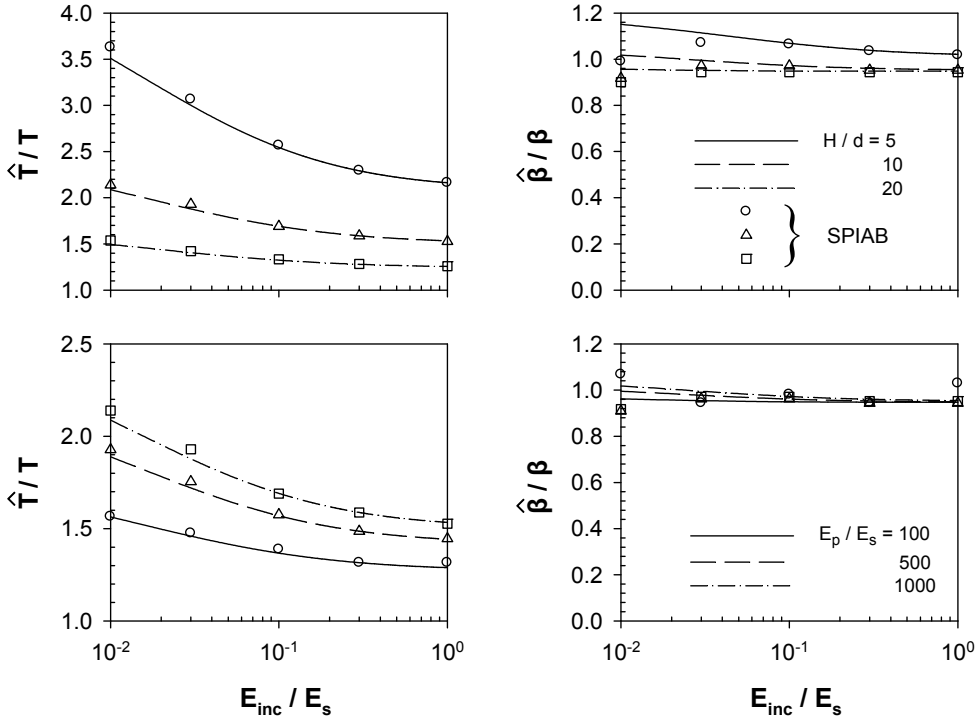

Figure 4: System period and effective damping as function of inclusion-soil stiffness ratio E_{inc}/E_s: Influence of slenderness ratio H/d and pile-soil stiffness contrast E_p/E_s.

5 TIME-DOMAIN ANALYSES

5.1 Parameters investigated

The aim of this section is to examine the effect of the inclusion around the pile to the base shear of the bridge-pier column and the maximum pile bending moment when the system is excited by an actual earthquake. To this end, two acceleration records (Takatori 1995, Lefkada 2003) with different peak ground acceleration and frequency content are utilized, with the excitation described through a horizontal rock "outcrop" motion. Takatori (M_w = 6.9, T_c = 1.25 sec, PGA = 0.61 g) and Lefkada (M_w = 6.3, T_c = 0.56 sec, PGA = 0.34 g) earthquake records and the corresponding 5 per cent-damped response spectra are plotted in Fig. 5.

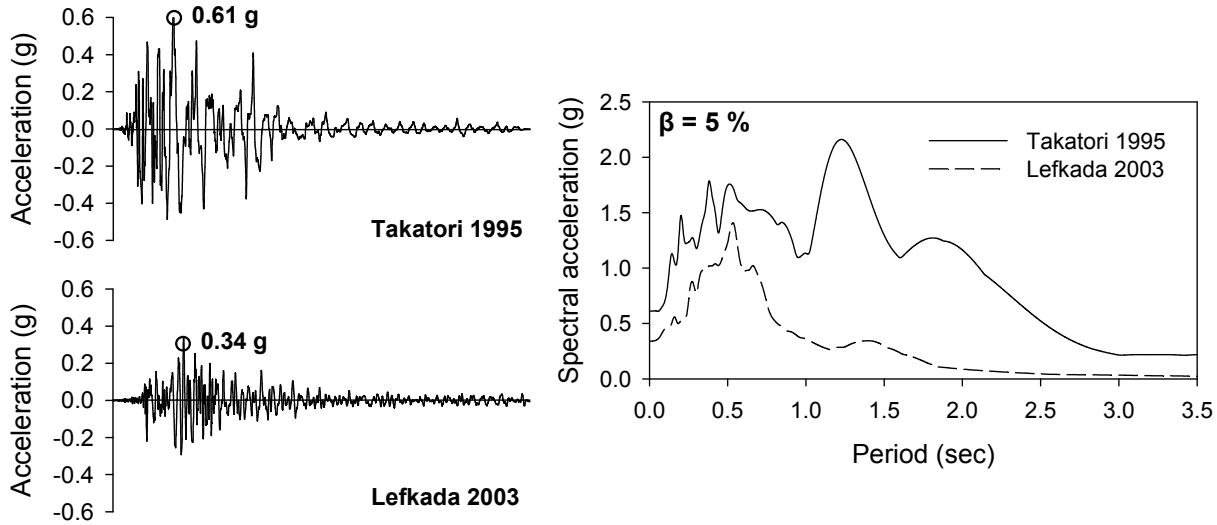

Figure 5: The two earthquake records used in the analyses and the corresponding 5 per cent – damped spectra.

A wide class of single-degree-of-freedom systems is excited using the two time-histories. For normalization purposes, the resonance ratio T/T_c is utilized, with T being the fixed-base natural frequency of the system and T_c the dominant period of excitation motion. The values T/T_c = 0.1, 0.2, 0.4, 0.5, 0.6, 0.8, 1.0, 1.2, 1.4, 1.5 are examined, which corresponds to ten different oscillators excited per time-history. Assuming that the bending stiffness K ($=3EI/H^3$) of the oscillator is kept constant, the mass m ($=(T/2\pi)^2K$) should be adjusted according to the T/T_c ratio.

Regarding geofoam properties, it is assumed that E_{inc}/E_s = 0.03 and the material damping ratio β_{inc} = 10%. The effect of thickness and length of EPS foam on the pier response is investigated. The pile-soil stiffness contrast is E_p/E_s = 1000 and two values for the dimensionless pier height (H/d =5, 10) are examined.

Time-domain results are obtained by means of computer code SPIAB [17]. For completeness, both kinematic interaction and radiation damping effect have been taken into account.

5.2 Change in base shear and pile bending moment

Results are presented in the form of dimensionless graphs. The ratios $S_A(\hat{T})$ / $S_A(\tilde{T})$ and $M_{max}(\hat{T})$ / $M_{max}(\tilde{T})$ refer to the base shear of the bridge-pier column and the maximum pile bending moment, respectively. In the above representation, the numerator refers to the bridge-pier-pile-inclusion-soil system, while the denominator to the bridge-pier-pile-soil system, ac-

counting solely for the effect of inclusion. Seismic forces are depicted in Figs. 6 and 8 as a function of the resonance ratio T / T_c. From Figs. 6 and 8, the following noteworthy trends are evident:

- A substantial decrease of the order of 20 to 70% in base shear and maximum pile bending moment for squat piers ($H / d = 5$) having $T / T_c \geq 0.4$, is observed. As anticipated, due to period elongation the system experiences lower spectral acceleration.
- For low resonance ratios the base shear is magnified, even doubled in some cases. This is also anticipated, since the elongated period of a system with an already short fundamental period falls in most of the cases within the region of high spectral accelerations in the input motions (Fig. 2).
- Analogous observations can be made for the maximum pile bending moment.
- An increase in D_e / L_a ratio marginally affects the variation in seismic forces. Instead, the increase in t / d ratio further reduces the seismic forces for $T / T_c \geq 0.4$, while it suppresses the response of the system for $T / T_c < 0.4$.
- Tall slender piers ($H / d = 10$) having $T / T_c \geq 0.6$ and EPS coat properties $t / d = 1$, $D_e / L_a = 1$, exhibit good performance for both excitations. The limited efficiency of the proposed method in tall slender piers is expected, since the response of such structures is controlled by the rocking component.

The distribution with depth of pile bending moments is plotted in Figs. 7 and 9. Results are presented for both pier-pile-soil system and pier-pile-EPS-soil system. The total pile bending moment M is normalized with the peak value $M_{max}(\tilde{T})$ developed in the pile when there is no EPS coat around it, while the depth in the vertical axis is normalized with the pile diameter d. The following interesting observations can be made:

- The inclusion around the pile leads to a considerable decrease in total pile bending moment. Apart from the decrease in magnitude, the distribution with depth of bending moments changes drastically. Recall to this end that pile deformations due to inertial forces transmitted from the superstructure attenuate rapidly with depth and practically vanish below the depth of active pile length. Indeed, in the case of no EPS coat bending moment almost vanishes below $z \cong 7.8$m ($d = 1$). With EPS coat, the active pile length increases to $L_a \cong 13.7$m and the bending moment becomes negligible below that depth.
- The depth of peak pile bending moment moves deeper and the amount of this variation depends on pile-soil and inclusion relative compliances.
- Evidently, the decrease in pile bending moment is larger for a squat pier than a slender one. The positive influence of EPS coat is observed for squat piers and systems having $T/T_c \geq 0.5$, and for tall piers and systems with $T / T_c \geq 1.0$.
- For $T / T_c = 0.2$, the EPS coat suppresses the pile bending moments. In that case, kinematic bending moment seems to dominate. This is anticipated, since the mass of the superstructure is small and, thus, the inertial loads are negligible compared to kinematic ones.

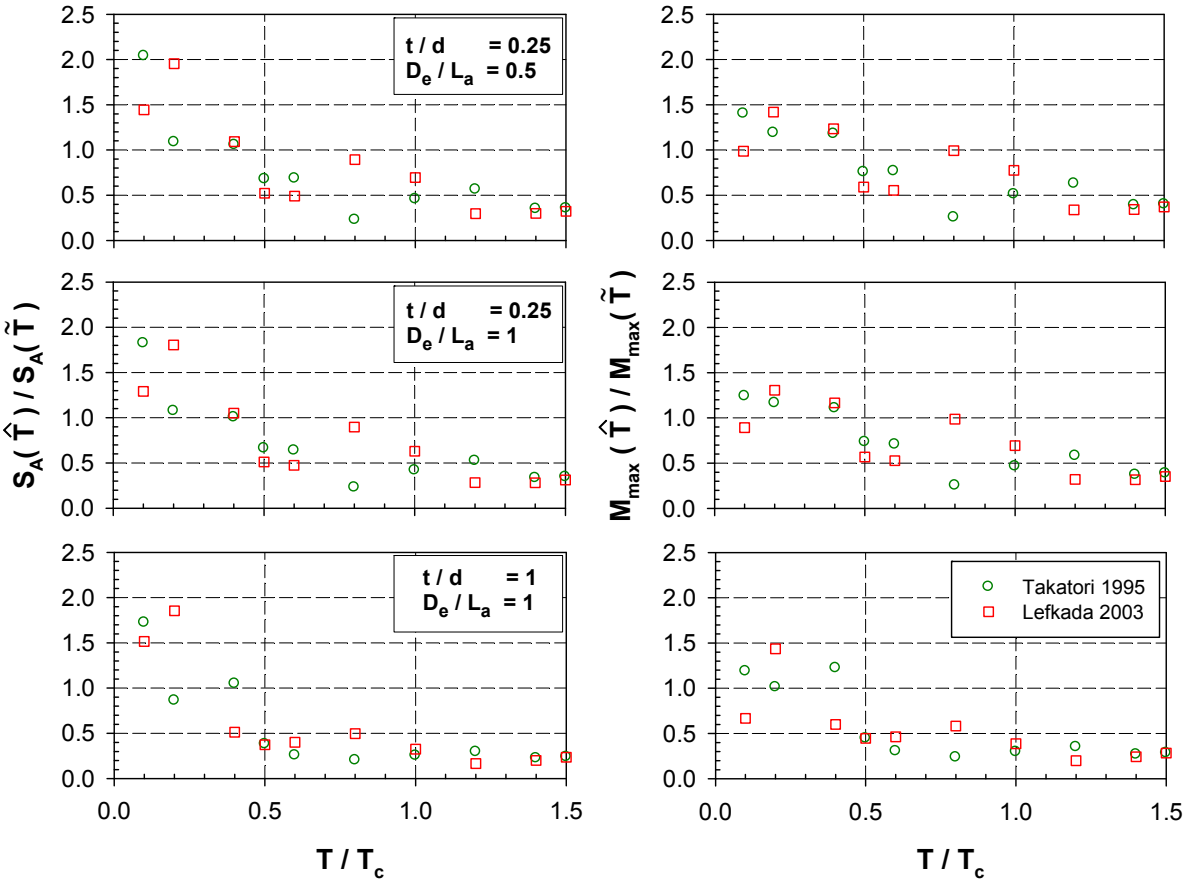

Figure 6: Normalized results for base shear force and maximum bending moment for squat piers (H/d = 5) as a function of resonance ratio T/T_c; $E_p/E_s = 1000$, $E_{inc}/E_s = 0.03$, $\beta_{inc} = 0.10$.

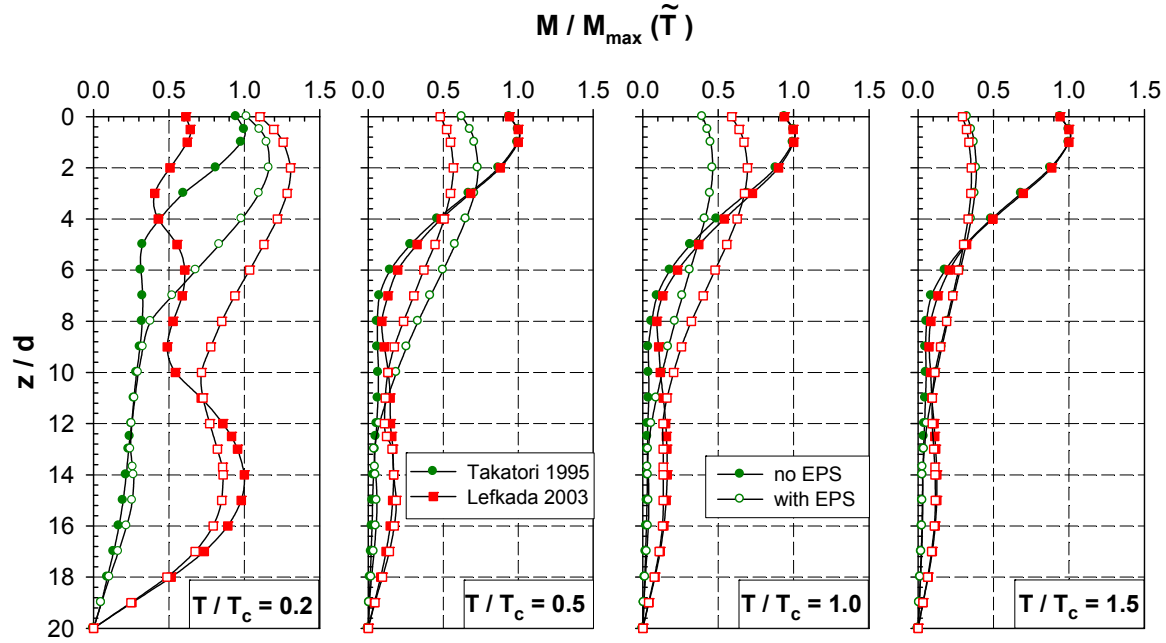

Figure 7: Distribution with depth of normalized pile bending moment for resonance ratios $T/T_c = 0.2$, 0.5, 1.0, 1.5; H/d = 5, $E_p/E_s = 1000$, t/d = 0.25, $D_e/L_a = 1$, $E_{inc}/E_s = 0.03$, $\beta_{inc} = 0.10$.

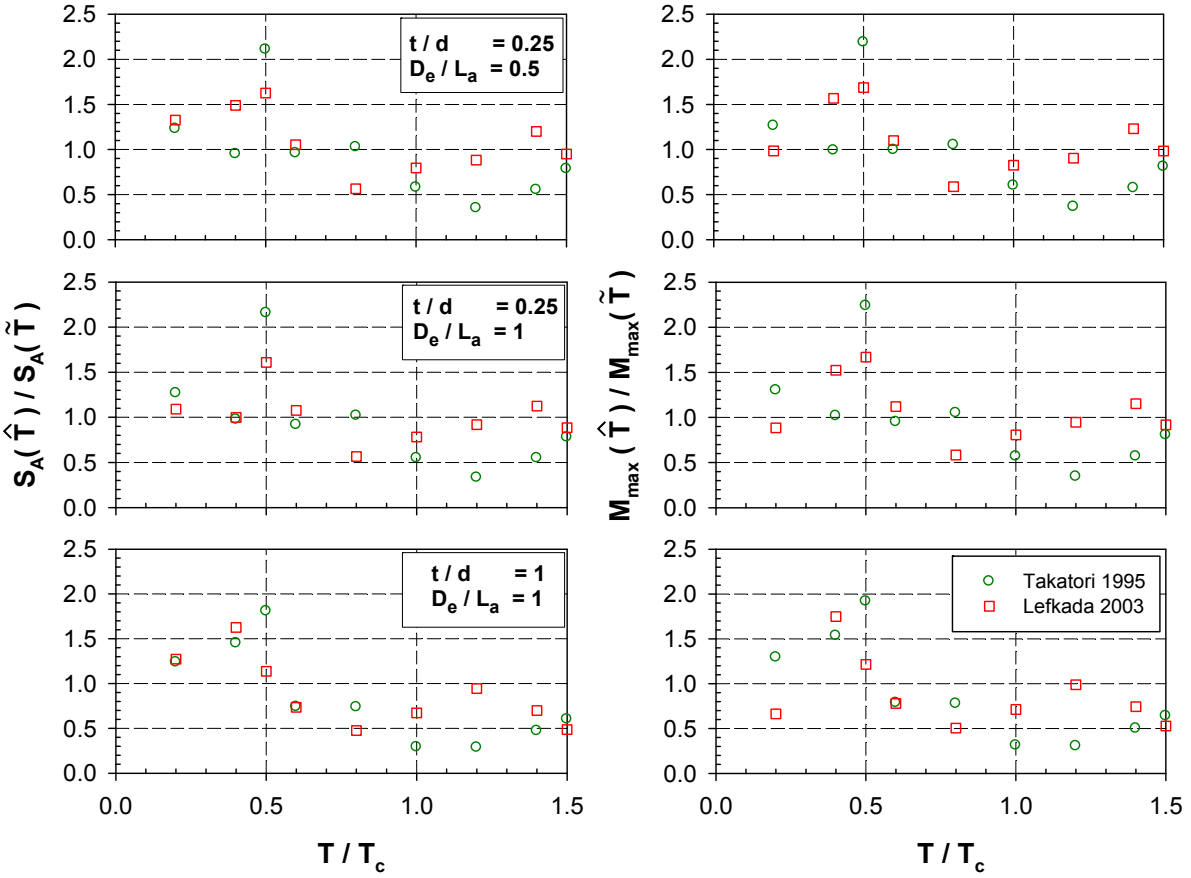

Figure 8: Normalized results for base shear force and maximum bending moment for high piers (H/d = 10) as a function of resonance ratio T/T_c; $E_p/E_s = 1000$, $E_{inc}/E_s = 0.03$, $\beta_{inc} = 0.10$.

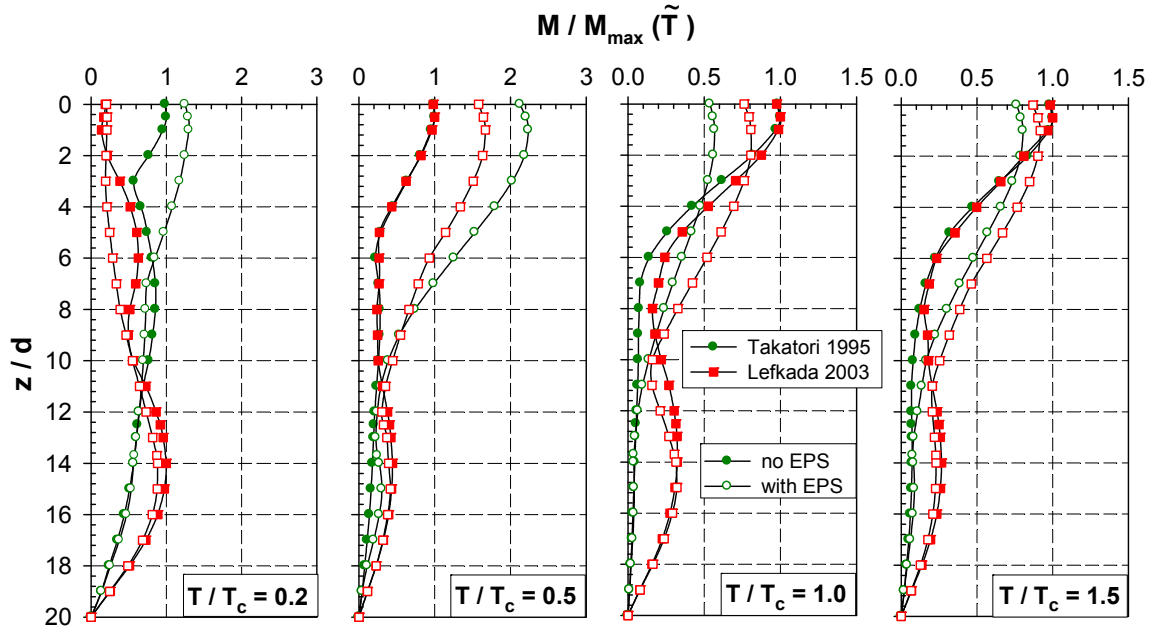

Figure 9: Distribution with depth of normalized pile bending moment for resonance ratios $T/T_c = 0.2$, 0.5, 1.0, 1.5; H/d = 10, $E_p/E_s = 1000$, t/d = 0.25, $D_e/L_a = 1$, $E_{inc}/E_s = 0.03$, $\beta_{inc} = 0.10$.

5.3 Change in total bridge deck displacement

Regarding the isolation methods, as it has already mentioned, there is a concern about the potential for high residual displacements. Due to increase in flexibility of the system, the fundamental period is shifted in or near the displacement-sensitive region of the spectrum. The pertinent time-domain analysis reveals a considerable increase in bridge deck deformation. In this regard, Fig. 10 depicts results for the total displacement of the bridge deck in case that the systems T / T_c = 0.2, 0.5, 1, 1.5 are subjected to the extreme Takatori seismic excitation. It is shown that, with exception of the system with T / T_c = 1.5, the use of EPS coat increases the overall deck deformation relative to the overall deck deformation without considering EPS by about 1.4, 1.05 and 1.13. For T/T_c = 1.5, it is observed that the displacement is reduced by half.

Evidently, the change in structural displacements and the magnitude of deformations is not known a priori. This indicates that the application of the proposed isolation method should be accompanied by a check of structural displacements to be within acceptable limits.

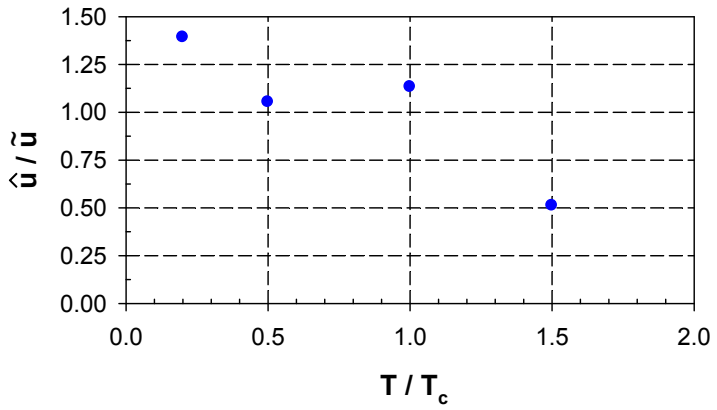

Figure 10: Normalized total displacement of the bridge deck upon Takatori excitation; H/d = 5, E_p/E_s = 1000, E_{inc}/E_s = 0.03, t/d = 0.25, D_e/L_a = 0.5, β_{inc} = 0.10.

6 CONCLUSIONS

A novel geotechnical isolation method for the seismic protection of pile-supported bridge piers was presented. The proposed method uses EPS geofoam around the piles and provides an efficient means of simple and inexpensive seismic isolation. An analysis framework for a bridge pier supported on a single pile enhanced with EPS coat was developed based on pertinent Winkler considerations of soil reaction. Through a simplified analytical solution, the fundamental period and the effective damping of the pier-foundation system were derived. Theoretical investigation showed that EPS coat around the pile acts as an elementary base-isolation mechanism increasing the flexibility of the system and, hence, the fundamental period of the pier. Regarding the vibrational properties of the pier, comparison between the proposed analytical solution and the numerically evaluated results from the computer code SPIAB is excellent. The most significant findings obtained from the time-domain analyses are:

a) For squat piers (H / d = 5) with resonance ratio $T / T_c \geq 0.4$, a substantial decrease, about 20 to 70%, in base shear and associated maximum bending moment are observed. On the other hand, for $T / Tc < 0.4$, the base shear increases.
b) The presence of the EPS coat leads to a considerable decrease in pile bending moment and changes its distribution with depth, with the point of peak bending moment moving downward.
c) The proposed method seems to have limited impact on tall slender piers (H / d = 10). The positive effect of EPS is observed for systems having resonance ratio $T / T_c \geq 0.6$.

d) The change in the magnitude of pier displacements is hard to determine a priori and careful checks are needed.

7 APPENDIX

In Eqs. (14) and (15), parameters $\chi_1, \chi_2, \chi_3, \chi_4, \chi_5, \chi_6, \chi_7$ are

$$\chi_1 = \frac{HK_{hh}}{K_{hr}}\left(1+4\beta_{hh}^2\right) \quad , \quad \chi_2 = \frac{K_{rr}}{HK_{hr}}\left(1+4\beta_{rr}^2\right) \quad , \quad \chi_3 = -1+4\beta_{hh}\beta_{rr} \quad , \quad \chi_4 = \beta_{hh}+\beta_{rr} \tag{21}$$

$$\chi_5 = 2\left(1+4\beta_{hr}^2\right) \quad , \quad \chi_6 = \frac{HK_{hh}}{K_{hr}}\beta_{hh} + \frac{K_{rr}}{HK_{hr}}\beta_{rr} \quad , \quad \chi_7 = \frac{HK_{hh}}{K_{hr}} + \frac{K_{rr}}{HK_{hr}} \tag{22}$$

REFERENCES

[1] H.H. Tsang, Geotechnical Seismic Isolation in Earthquake Engineering: New Research. *Nova Science Publishers*, Inc., New York, U.S., 55-87, 2009.

[2] E. Jr. Kavazanjian, B. Hushmand, G. R. Martin, Frictional base isolation using a layered soil-synthetic liner system. *Proc., 3rd U.S. Conf. on Lifeline Earthquake Engrg.*, *ASCE*, New York, N.Y., 1140 – 1151, 1991.

[3] M. Yegian, A. Lahlaf, Dynamic Interface Shear Strength Properties of Geomembranes and Geotextiles. *Journal of Geotechnical Engineering*, 10.1061/(ASCE)0733-9410(1992)118:5(760), 760-779, 1992.

[4] M.K. Yegian, U. Kadakal, Foundation Isolation for Seismic Protection Using a Smooth Synthetic Liner. *Journal of Geotechnical and Geoenvironmental Engineering*, **130**(11), 1121-1130, 2004.

[5] M. Yegian, M. Catan, Soil Isolation for Seismic Protection Using a Smooth Synthetic Liner. *J. Geotech. Geoenviron. Eng.*, 10.1061/(ASCE)1090-0241(2004)130:11(1131), 1131-1139, 2004.

[6] H.H. Tsang, Seismic isolation by rubber-soil mixtures for developing countries. *Earthquake Engineering and Structural Dynamics*, **37**(2), 283-303, 2008.

[7] W. Xiong, H. H. Tsang, S. H. Lo, S. P. Shang, H.D. Wang, F. Y. Zhou, Geotechnical Seismic Isolation System - Experimental Study. *Advanced Materials Research*, 163-167, 4449-4453, 2010.

[8] W. Xiong, M. R. Yan, Y. Z. Li, Geotechnical Seismic Isolation System – Further Experimental Study. *Applied Mechanics and Materials*, 580-583, 1490-1493, 2014.

[9] J.S. Horvath, Geofoam Geosynthetic. *Horvath Engineering*, P.C. Scarsdale, New York, USA, 217 p., 1995.

[10] G.A. Athanasopoulos, P.C. Pelekis, V.C. Xenaki, Dynamic Properties of EPS Geofoam: An Experimental Investigation. *Geosynthetics International*, **6**(3), 171-194, 1999.

[11] P. Papastylianou, *Seismic Isolation of Pile Supported Bridge Piers with EPS Geofoam*. Ph.D. Dissertation University of Patras, Greece, 2010.

[12] M. Novak, M. Sheta, Approximate approach to contact effects of piles. *Proc. Dynamic Response of Pile Foundations: Analytical Aspects, ASCE*, New York, 53–79, 1980.

[13] X. Karatzia, P. Papastylianou, G. Mylonakis, Horizontal Soil Reaction of a Cylindrical Pile Segment with a Soft Zone. *Journal of Engineering Mechanics*, 10.1061/(ASCE)EM. 1943-7889.0000792, 04014077, 2014.

[14] C. Syngros, *Seismic response of piles and pile-supported bridge piers evaluated through case histories*. PhD Thesis, The City College and the Graduate Center of the City University of New York, 2004.

[15] G. Gazetas, R. Dobry, Horizontal response of piles in layered soils. *J. Geotech. Eng. Div., ASCE*, 110, 20-40, 1984.

[16] X. Karatzia, G. Mylonakis, Horizontal stiffness and damping of piles in inhomogeneous soil. *J. Geotech. Geoenviron*. Eng. DOI:10.1061/(ASCE)GT.1943-5606.0001621, 2016.

[17] G. Mylonakis, *Contributions to the static and seismic analysis of pile and pile-supported bridge pier*. Ph.D. Dissertation, State University of New York, 1995.

[18] R. Di Laora, E. Rovithis, Kinematic bending of fixed-head piles in nonhomogeneous soil. *J. Geotech. Geoenviron. Eng.* **141**(4) 04014126, DOI: 10.1061/(ASCE) GT.1943-5606.0001270, 2015.

[19] G. Mylonakis, D. Roumbas, Lateral impedance of single piles in inhomogeneous soil. *4th Int. Conf. on Recent Advances in Geotech. Earthquake Eng. and Soil Dyn.*, San Diego, 2001.

[20] NIST, *Soil-Structure Interaction for Building Structures*, GCR 12-917-21, prepared by the NEHRP Consultants Joint Venture, a partnership of the Applied Technology Council and the Consortium for Universities for Research in Earthquake Engineering, for the National In-stitute of Standards and Technology, Gaithersburg, MD, 2012.

[21] V. Zania, Natural vibration frequency and damping of slender structures founded on monopiles. *Soil Dynamics and Earthquake Engineering*, **59**, 8-20, 2014.

[22] X. Karatzia, *Theoretical investigation of geotechnical seismic isolation of bridge piers on footings and piles*. Ph.D. Dissertation, University of Patras, Greece, 2016.

[23] X. Karatzia, G. Mylonakis, Geotechnical Isolation of Pile-Supported Bridge Piers using EPS Geofoam. *16th World Conference on Earthquake Engineering (16th WCEE 2017)*, Santiago Chile, No. 2278, 2017.

[24] B. Bradley, Period Dependence of Response Spectrum Damping Modification Factors due to Source- and Site-Specific Effects, *Earthquake Spectra*, 10.1193 /070213EQS189M, 745-759, 2015.